Received: 14 June 2021 | Accepted: 9 July 2021

DOI: 10.1111/gcb.15801

PRIMARY RESEARCH ARTICLE

Global Change Biology WILEY

Divergent responses of primary production to increasing precipitation variability in global drylands

Enqing Hou[1] | Marcy E. Litvak[2] | Jennifer A. Rudgers[2] | Lifen Jiang[1] | Scott L. Collins[2] | William T. Pockman[2] | Dafeng Hui[3] | Shuli Niu[4] | Yiqi Luo[1]

[1]Center for Ecosystem Science and Society, Department of Biological Sciences, Northern Arizona University, Flagstaff, Arizona, USA

[2]Department of Biology, MSC03-2020, University of New Mexico, Albuquerque, New Mexico, USA

[3]Department of Biological Sciences, Tennessee State University, Nashville, Tennessee, USA

[4]Key Laboratory of Ecosystem Network Observation and Modeling, Institute of Geographic Sciences and Natural Resources Research, Chinese Academy of Sciences, Beijing, China

Correspondence
Enqing Hou and Yiqi Luo, Center for Ecosystem Science and Society, Department of Biological Sciences, Northern Arizona University, Flagstaff, AZ, USA.
E-mail: houeq@scbg.ac.cn; yiqi.luo@nau.edu

Funding information
National Science Foundation for Long-term Ecological Research, Grant/Award Number: 1748133 and 1655499

Abstract

Interannual variability in precipitation has increased globally as climate warming intensifies. The increased variability impacts both terrestrial plant production and carbon (C) sequestration. However, mechanisms driving these changes are largely unknown. Here, we examined mechanisms underlying the response of aboveground net primary production (ANPP) to interannual precipitation variability in global drylands with mean annual precipitation (MAP) <500 mm year^{-1}, using a combined approach of data synthesis and process-based modeling. We found a hump-shaped response of ANPP to precipitation variability along the MAP gradient. The response was positive when MAP < ~300 mm year^{-1} and negative when MAP was higher than this threshold, with a positive peak at 140 mm year^{-1}. Transpiration and subsoil water content mirrored the response of ANPP to precipitation variability; evaporation responded negatively and water loss through runoff and drainage responded positively to precipitation variability. Mean annual temperature, soil type, and plant physiological traits all altered the magnitude but not the pattern of the response of ANPP to precipitation variability along the MAP gradient. By extrapolating to global drylands (<500 mm year^{-1} MAP), we estimated that ANPP would increase by 15.2 ± 6.0 Tg C year^{-1} in arid and hyper-arid lands and decrease by 2.1 ± 0.5 Tg C year^{-1} in dry sub-humid lands under future changes in interannual precipitation variability. Thus, increases in precipitation variability will enhance primary production in many drylands in the future.

KEYWORDS
aboveground net primary production, data synthesis, drylands, mean annual precipitation, precipitation variability, process-based model

1 | INTRODUCTION

Precipitation has become increasingly variable in the past century and will become more so in the coming decades due to climate warming (Seneviratne et al., 2012; Stocker, 2013). This increased variability can affect ecosystem services such as primary production (Gherardi & Sala, 2019; Hsu et al., 2012; Knapp et al., 2008; Liu et al., 2020; Seneviratne et al., 2012), and can also drive state change in alternative stable state systems (Borgogno et al., 2007; Chen et al., 2018). Drylands are among the most sensitive ecosystems to precipitation variability globally (Ahlström et al., 2015; Gherardi & Sala, 2019; Haverd et al., 2017). Moreover, drylands occupy ~45% of the global land surface, support nearly 40% of the world's population, and contribute significantly to the interannual variability in global primary production (Haverd et al., 2017; Maurer et al., 2020; Poulter et al., 2014; Prăvălie, 2016). Therefore, it is imperative to investigate the effects of increased precipitation variability on dryland primary production (Gherardi & Sala, 2019;

Haverd et al., 2017; Knapp et al., 2017; Luo et al., 2017; Rudgers et al., 2018).

The effect of precipitation variability on primary production has been increasingly investigated during the past two decades, but mostly at intra-annual time scales (i.e., the event size or seasonality of precipitation) (Heisler-White et al., 2009; Knapp et al., 2002, 2008; Liu et al., 2020; Meng et al., 2021; Thomey et al., 2011) and much less at interannual time scales (i.e., year-to-year variation) (Gherardi & Sala, 2019; Haverd et al., 2017; Liu et al., 2020; Rudgers et al., 2018). Theory, manipulative experiments, and observations all generally suggest a positive effect of intra-annual precipitation variability on aboveground net primary production (ANPP) in xeric ecosystems and a negative effect in mesic ecosystems, with a mean annual precipitation (MAP) threshold between 300 and 650 mm $year^{-1}$ (Heisler-White et al., 2008, 2009; Knapp et al., 2002, 2008; Liu et al., 2020; Thomey et al., 2011). Recently, Gherardi and Sala (2019) estimated the effect of interannual precipitation variability on ANPP as the slope of the regression line between the mean of ANPP and the coefficient of variation (*CV*) of annual precipitation in 5-year moving windows at 43 globally distributed sites, where long-term ANPP observations were available. They found that the effect increased linearly with decreasing MAP and switched from negative to positive at 300 mm $year^{-1}$, with the largest positive effect at the driest sites. However, their global synthesis included only one site under very dry conditions (i.e., MAP < 230 mm $year^{-1}$), thus further analysis of low precipitation sites is needed. In fact, ANPP is hypothesized to be relatively insensitive to precipitation change at very dry sites, due to meristem constraints and little infiltration of precipitation into soil (Hsu et al., 2012; Hu et al., 2018; Reichmann et al., 2013). Moreover, the regression approach used by Gherardi and Sala (2019) does not account for the influence of possible covariates (e.g., mean annual temperature (MAT)), and thus this observation requires further testing, as argued by Liu et al. (2020). Indeed, using a different statistical method on a similar dataset, Hsu et al. (2012) found minor effects of interannual precipitation variability on ANPP at 58 globally distributed sites. To date, only one long-term (i.e., 6-year) experiment has experimentally manipulated interannual precipitation variability, finding an initial negative, rather than a positive, effect on ANPP in a xeric grassland with ~240 mm $year^{-1}$ MAP (Gherardi & Sala, 2015).

The shift in the effect of precipitation variability on ANPP along the MAP gradient is usually explained by a hydrological hypothesis (Gherardi & Sala, 2019; Heisler-White et al., 2008, 2009; Thomey et al., 2011), which states that large precipitation events penetrate deeper into the soil profile. Subsoil water in xeric systems is depleted mostly by transpiration and less so by evaporative losses. In contrast, in mesic ecosystems, theory predicts that large precipitation events can increase water loss through runoff and drainage, resulting in lower soil water availability per rain event (Knapp et al., 2008). Although frequently inferred, this soil moisture hypothesis has been infrequently tested or tested with only surface soil water content measurements (Gherardi & Sala, 2019; Heisler-White et al., 2008, 2009; Thomey et al., 2011), without any measurements of evaporation, transpiration, infiltration, runoff, or drainage, due to operational challenges.

This hydrological mechanism is even harder to test empirically at interannual time scales, when antecedent or legacy effects of precipitation may be a factor (Reichmann et al., 2013; Sala et al., 2012). Nevertheless, the mechanism can be investigated using a process-based model that can incorporate a wide range of scenario settings (Liu et al., 2020; Sala et al., 2015). For example, using a process-based hydrological model, Sala et al. (2015) found that the effects of interannual precipitation variability on soil water availability and transpiration were positive when MAP < 380 mm $year^{-1}$ (ranged between 350 and 440 mm $year^{-1}$) and negative at higher values of MAP. While the results generally supported the hydrological mechanism, the model used did not consider water losses through runoff nor was it validated by any measurement at the simulated sites. Moreover, the hydrological model did not include any C cycle representation and therefore provides only partial insight into the effects of precipitation variability on the C cycle.

In addition to MAP, the effect of precipitation variability on ANPP may be also modulated by MAT, soil type, vegetation type, as well as the variability patterns (i.e., magnitude, duration, and stochasticity) and antecedent effects of precipitation (Felton et al., 2021; Liu et al., 2020; Rudgers et al., 2018; Sala et al., 2012). For example, an ecosystem with high MAT loses more water from surface soil through evaporation, and therefore may benefit more from the percolation of large precipitation events to deep soil than an ecosystem with lower MAT where evaporation is less (Liu et al., 2020). Sandy soils facilitate infiltration and therefore may benefit more from increased precipitation variability under low MAP, but can lose more water under high MAP due to lower water holding capacity, in comparison to loamy or clay soils (Sala et al., 1988, 2015). Vegetation type can modulate the effect of precipitation variability on ANPP through plant physiological properties that are closely related to plant uptake and utilization of water, such as leaf growth rate and soil-profile root distribution (Rudgers et al., 2018; Xu et al., 2015). For example, a fast growth rate allows plants to rapidly increase biomass when water is available and therefore may benefit from increased soil water availability under variable precipitation at dry sites (Rudgers et al., 2018; Xu et al., 2015). Deep roots benefit from increased precipitation variability due to deep penetration of large precipitation events into soil (Gherardi & Sala, 2015).

Although a number of mechanisms have been proposed to explain the effect of precipitation variability on ANPP, most of the mechanisms have been tested at only a small number of sites (Gherardi & Sala, 2015; Heisler-White et al., 2008, 2009; Liu et al.,

2020; Rudgers et al., 2018). Whether these mechanisms can be generalized is unclear, and the relative importance of each mechanism under broad environmental conditions remains poorly understood. This knowledge gap needs to be filled in order to predict dryland primary production in response to future changes in precipitation variability at regional to global scales.

We investigated the effect of interannual precipitation variability (hereafter *precipitation variability*) on ANPP in global drylands (outlined by UNEP-WCMC (2007)) with MAP < 500 mm year^{-1}, using a combined approach of data synthesis and modeling. We focused on these drylands because of their high precipitation variability (Knapp, Hoover, et al., 2015) and high sensitivity to annual precipitation (Huxman et al., 2004; Maurer et al., 2020). In addition, drylands with MAP < 230 mm year^{-1} have been less studied (Gherardi & Sala, 2019; Hsu et al., 2012), despite accounting for 15.1% of global land surface. For data synthesis, we compiled a database of long-term (≥10 years) ANPP measurements from 43 globally distributed dryland sites, to explore the empirical relationship between the effect of precipitation variability on ANPP and MAP. Next, we conducted 8,330 long-term (i.e., 50 years) precipitation manipulation experiments using the process-based Terrestrial ECOsystem (TECO) model (Weng & Luo, 2008), to see whether the model can reproduce the empirical relationship, and to explore the underlying mechanisms. Finally, we extrapolated both the observed effects of precipitation variability on ANPP (using a machine learning approach) and the simulated ones to global drylands with MAP < 500 mm year^{-1}, to reveal global patterns of precipitation variability on ANPP.

We hypothesized that the effect of precipitation variability on ANPP would (1) show a unimodal relationship with MAP, (2) be modulated by MAT, soil type, and vegetation type, and (3) be explained mainly by how precipitation is partitioned into transpiration for plant growth versus loss through evaporation, runoff, and drainage. By testing these hypotheses, we can improve our understanding of the response of dryland ANPP to precipitation variability and the underlying mechanisms, and therefore gain a more predictive understanding of ANPP dynamics under future increases in precipitation variability.

2 | METHODS

2.1 | Data synthesis

We synthesized long-term (≥10 years) ANPP measurements in drylands to estimate the effect of interannual precipitation variability on ANPP. The long-term ANPP datasets were compiled by searching EcoTrends database (EcoTrends database, 2004), the Oak Ridge National Laboratory Distributed Active Archive Center (ORNL DAAC) database (Oak Ridge National Laboratory Distributed Active Archive Center, 2009), Long Term Ecological Research (LTER) database (Long Term Ecological Research Network, 2016), and google scholar using the keyword of "ANPP" or "above-ground net primary production." To be included in our database, the site or the ANPP measurements had to meet all of the following criteria. (1) Site was a dryland with MAP < 500 mm year^{-1} that has not had significant human disturbance, that is, no fertilization, irrigation, anthropogenic fire regime, or land use change history. Grasslands that have been slightly, but not moderately or heavily, grazed were included. (2) ANPP was measured for at least 10 years, and annual (calendar) precipitation in the corresponding years was available or could be reliably derived from nearby weather stations. Multiple ecosystems with different vegetation types or locations at the same research station were taken as multiple sites.

In total, we compiled long-term ANPP measurements from 43 globally distributed drylands with MAP < 500 mm year^{-1}, including 35 grasslands, 7 shrublands, and 1 savanna (Figure 1a; Table S1). Our database included all 29 sites with MAP < 500 mm yr^{-1} in Gherardi and Sala (2019) as well as another 14 sites. For each site, we have also recorded geographic location (i.e., latitude and longitude), elevation, MAT, and soil particle size measurements when available. We have filled missing values of MAT (53.5%) and soil particle size (83.7%) by values derived from WorldClim (Fick & Hijmans, 2017) and HWSD databases (Wieder et al., 2014), respectively, using site geographic location.

We used precipitation SD rather than precipitation CV to represent precipitation variability (Figure 1), because the SD, but not the CV, of annual precipitation was less dependent on MAP across

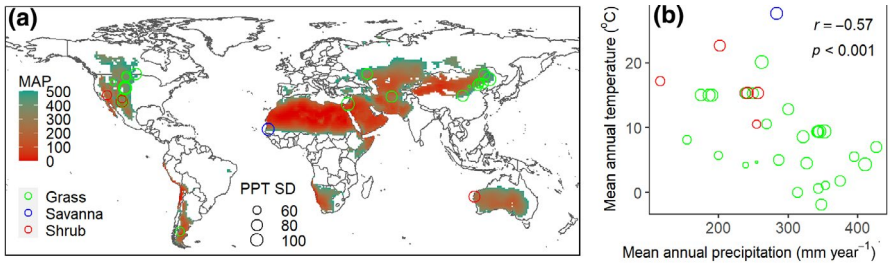

FIGURE 1 Distribution of drylands with mean annual precipitation (MAP) of <500 mm year^{-1}. (a) Geographical distributions of global drylands with MAP < 500 mm year^{-1} (color filled), and the 43 dryland sites (circles) where long-term aboveground net primary production measurements were obtained for this study. (b) Climatological distribution of the 43 dryland sites along MAP and mean annual temperature gradients. Circle size is proportional to the standard deviation of annual precipitation (PPT SD, mm year^{-1}) [Colour figure can be viewed at wileyonlinelibrary.com]

sites (SD: $r = 0.30$, $p = 0.054$; CV: $r = -0.76$, $p < 0.001$). We aggregated the synthesized data at each site in 5-year moving windows and calculated the mean of ANPP and the SD of annual precipitation for each time window. We then constructed a linear relationship between the 5-year moving ANPP mean (*Y* axis) and precipitation SD (*X* axis) at each site. Slope of the linear regression line at each site was used to quantify the effect of precipitation variability on ANPP. The slope was regressed against MAP using a sample size-weighted regression approach to quantify the relationship between the effect of precipitation variability on ANPP and MAP.

2.2 | Model simulations

We performed model simulations with the TECO model (Jiang et al., 2018; Weng & Luo, 2008) for four purposes. One was to explore whether the model can reproduce the observed effect of precipitation variability on ANPP along the MAP gradient. The second purpose was to extend the relationship to very dry conditions (i.e., MAP < 230 mm year^{-1}) where long-term ANPP observations were rare (Table S1). The third purpose was to explore the hydrological mechanisms underlying ANPP response to precipitation variability along the MAP gradient (Gherardi & Sala, 2019; Sala et al., 2015). The fourth purpose was to explore whether and how MAT, soil type, and vegetation type would modulate the effect of precipitation variability on ANPP.

The TECO model has proven to be a useful tool to examine the responses of terrestrial C and water cycles to multiple global change factors (e.g., precipitation) in diverse ecosystems (e.g., grasslands, shrublands, and forests) (Jiang et al., 2018; Paschalis et al., 2020; Weng & Luo, 2008). The TECO model is driven by six climate variables, including precipitation, wind speed, solar radiation, air temperature, relative humidity, and vapor pressure deficit. It couples terrestrial C, water, and energy dynamics at an hourly time step. The C cycle includes photosynthesis, C allocation, and C transformation (Weng & Luo, 2008). Leaf photosynthesis is based on the Farquhar model, which is mainly a function of leaf maximum carboxylation rate (V_{cmax}). Leaf photosynthetic rate is constrained by water supply through a roots-weighted soil water scaler. The soil is divided into 10 layers, with soil thickness of 5 cm for the first layer, 10 cm for the second layer, 15 cm for the third to fifth layers, and 20 cm for the sixth to tenth layers. The soil water subroutine simulates soil water content based on the balance between water inputs (precipitation) and outputs (evaporation, transpiration, runoff, and drainage). Evaporation depletes water from the topsoil (i.e., the first layer of soil). Transpiration depletes water from all soil layers where roots are present and is allocated to the soil layers based on the root fraction in each soil layer. The movement of water between adjacent soil layers is simulated based on unsaturated water flow (Ryel et al., 2002). More details about the TECO model can be seen in Text S1.

Before model simulations, we calibrated the TECO model with 8 years (2010–2017) of measurements of C, water, and energy dynamics in a desert grassland in the Sevilleta National Wildlife Refuge in New Mexico, U.S. (34.4 N, 106.7 W), the site of the Sevilleta LTER Program. The grassland is a typical dryland, where MAP (~250 mm year^{-1}) is in the middle of the MAP range we explored (20–500 mm year^{-1}), MAT (13.5°C) is in the middle of MAT range in drylands (typically be 0–25°C), and soil type (sandy loam) is common in drylands. Our model simulated well 8-year changes in C, water, and energy fluxes in the desert grassland (Figure S1; Table S2). This prototype served as a robust basis for the following model simulations.

To address the first two modeling purposes, we simulated the effect of precipitation variability on ANPP in four steps, as described below and illustrated in Figure S2. First, we generated 50-year climate data (including the six climate variables listed above) to drive our TECO model, with each year climate data were randomly selected from the 8-year climate data at the Sevilleta site. Second, we increased precipitation variability in the 50-year climate data while keeping MAP and other climate data constant. To do this, we increased precipitation in half of the 50 years and decreased precipitation in the other half of the 50 years with the same magnitude. The years in which precipitation was increased or decreased were selected randomly. The magnitude of precipitation change (i.e., increase or decrease) in a year was increased stepwise from 0 to 120 mm year^{-1} with a step of 2.5 mm year^{-1} by scaling all precipitation events in the year. This generated 49 precipitation scenarios with the same MAP but different interannual precipitation variabilities. Model simulations on this set of precipitation scenarios were used to estimate the effect of precipitation variability on ANPP at ~250 mm year^{-1} MAP, that is, calculated as the slope of the regression line between 50-year ANPP mean (*Y* axis) and precipitation SD (*X* axis).

Third, we changed MAP in the 49 precipitation scenarios by scaling all precipitation events with a scaling factor of 0.1, 0.2, 0.3, 0.4, 0.5, 0.6, 0.7, 0.8, 0.9, 1.0, 1.2, 1.4, 1.6, 1.8, 2.0, 2.2, or 2.4. Model simulations on this set of precipitation scenarios enabled us to explore the effect of precipitation variability on ANPP at sites with MAP ranging from ~20 to ~500 mm year^{-1}, assuming that MAP is the main predictor of the effect of precipitation variability on ANPP. Validation of this assumption is tested as our fourth modeling purpose, which is described as follows. Fourth, we repeated the above three steps 10 times in order to generate more robust estimates of precipitation variability effects. The above four steps of precipitation manipulations resulted in a total of 8330 precipitation scenarios, which were calculated as 49 precipitation variability scenarios (step 2) × 17 MAPs (step 3) × 10 replicates (step 4). We ran model simulations on each of the 8330 precipitation scenarios. Before each model simulation, we ran model spin-up for 50 years, which was long enough for ANPP to stabilize in the TECO model.

To address the third modeling purpose, we calculated the effect of precipitation variability on ecosystem water fluxes (including transpiration, evaporation, runoff, and drainage) and water availability in the soil profile from our model simulations using a method similar to the calculation of the effect of precipitation variability on ANPP. Water availability in each soil layer was calculated as the difference

in water input and output of the soil layer. Changes in water fluxes and soil-profile water availability along the MAP gradient were fitted with smooth curves.

Since our TECO model is an ecosystem model with climate, soil type, and vegetation type set according to the dryland selected for calibration, the above inferences are restricted to drylands with similar environmental conditions and ecosystem properties. Our inferences may be also applicable to other drylands, if MAP is the main predictor of the effect of precipitation variability on ANPP, as suggested in some previous studies (Gherardi & Sala, 2019; Liu et al., 2020). Whether and how MAT, soil type, and vegetation type (indexed by leaf V_{cmax} and soil-profile root distribution) would modulate the effect of precipitation variability on ANPP were explored as our fourth modeling purpose by changing these site properties in our TECO model. Specially, we changed MAT from 13.5°C (default) to 18.5°C, soil type from sandy loam soil (default) to loam soil (corresponding soil hydraulic properties in Table S3), leaf V_{cmax} (determines leaf photosynthesis rate in the model) from 80 μmol m^{-2} s^{-1} (default value) to 40 μmol m^{-2} s^{-1}, or soil-profile root distribution from the default setting to a deeper or a shallower root distribution (details in Table S4), and re-conducted model simulations on all 8,330 precipitation scenarios.

2.3 | Global patterns

At the global scale, we examined the spatial patterns of ANPP response to historical (1905–2010) and future (2010–2095) changes in precipitation variability in global drylands with MAP < 500 mm $year^{-1}$. The drylands were selected as the intersection of global drylands outlined by UNEP-WCMC (2007) and global lands with MAP < 500 mm $year^{-1}$, which has an area of 43.5 million km^2 and covers 29.2% of global land surface (Figure 1a).

In brief, ANPP change due to historical or future changes in precipitation variability was calculated as:

$$\text{Historical (or Future) ANPP change} = \text{VarChange}_{\text{historical}} \left(\text{or VarChange}_{\text{future}}\right) \times \text{VarEffect}_{\text{ANPP}},$$

where $\text{VarChange}_{\text{historical}}$ indicates the historical change in precipitation variability, which was calculated as the difference of precipitation SD between 1901–1910 and 2006–2015 (10-year windows) based on the Climatic Research Unit Time Series (CRU TS) dataset (Harris et al., 2014). $\text{VarChange}_{\text{future}}$ indicates the future change in precipitation variability, which was calculated as the difference of precipitation SD between 2006–2015 and 2090–2099 projected under RCP8.5 scenario by each of the nine Coupled Model Intercomparison Project Phase 5 (CMIP5) models (Table S5) (Taylor et al., 2012). Similar $\text{VarChange}_{\text{historical}}$ and $\text{VarChange}_{\text{future}}$ results were obtained when using 15-year or 20-year windows (results not shown). $\text{VarEffect}_{\text{ANPP}}$ indicates the effect of per unit precipitation SD on ANPP. It was either predicted from our model simulations with global MAP as the input or extrapolated from the observed effects at the 43 sites.

Observed-effect based $\text{VarEffect}_{\text{ANPP}}$ values were extrapolated to the global scale by a boosted regression tree (BRT) model. The BRT model took the observed effects of precipitation variability on ANPP at the 43 sites as the predicted values, site properties including MAP, MAT, vegetation type, and soil sand content and clay content as the predictors, and sample size as the weighting factor. Before constructing the final BRT model, we optimized model parameters (including bag fraction and learning rate). We set tree complexity to be 1, which indicates no interaction between predictors, due to a small sample size (Elith et al., 2008). To avoid model overfit, we pre-selected predictors by looking into the relative importance of all predictors. We found that vegetation type was of minor importance, and therefore excluded it from our final BRT model. For global extrapolation, we used MAP and MAT during 1951–2000 from CRU TS datasets (Harris et al., 2014), and soil sand content and clay content from HWSD database (Wieder et al., 2014) as model inputs. We performed all BRT analyses with the "gbm" package version 2.1.5 (Bivand & Piras, 2015) plus the custom code of another study (Elith et al., 2008) in R version 3.5.0 (R Core Team, 2020). Finally, we examined regional patterns by summing up the extrapolated ANPP response to historical or future changes in precipitation variability by aridity levels, that is, hyper-arid, arid, semi-arid, or dry sub-humid lands, defined according to UNEP-WCMC (2007).

The standard error of ANPP response to historical change in precipitation variability in each global grid or each aridity group was calculated based on two estimates, that is, (observed-effect or simulated-effect based $\text{VarEffect}_{\text{ANPP}}$) × historical change in precipitation variability. The standard error of ANPP response to future change in precipitation variability was calculated based on 18 estimates, that is, (observed-effect or simulated-effect based $\text{VarEffect}_{\text{ANPP}}$) × future change in precipitation variability projected by each of the nine CMIP5 models. All global spatial data were regridded into 1°×1° resolution if original data were not at that scale.

3 | RESULTS

3.1 | Observed effect of precipitation variability on ANPP

The observed effect of precipitation variability on ANPP varied from −0.29 to 0.21 (mean 0.02) g C m^{-2} mm^{-1} $year^{-1}$ across the 43 sites (Figure 2a). The effect decreased linearly with increasing MAP and switched from positive to negative at about 335 mm $year^{-1}$, both within grasslands and across all sites (R^2 = 0.14 and 0.13, respectively, $p < 0.05$; Figure 2a). Moreover, the effect of precipitation variability increased linearly with increasing MAT both within grasslands and across all sites excluding the only savanna, which had the highest MAT (27.6°C) (R^2 = 0.21 and 0.25, respectively, $p < 0.05$; Figure 2b). If the savanna site was included, the effect of precipitation variability on ANPP would show a unimodal relationship with MAT (R^2 = 0.26, p = 0.002; Figure 2b). The opposite changes in the effect along the

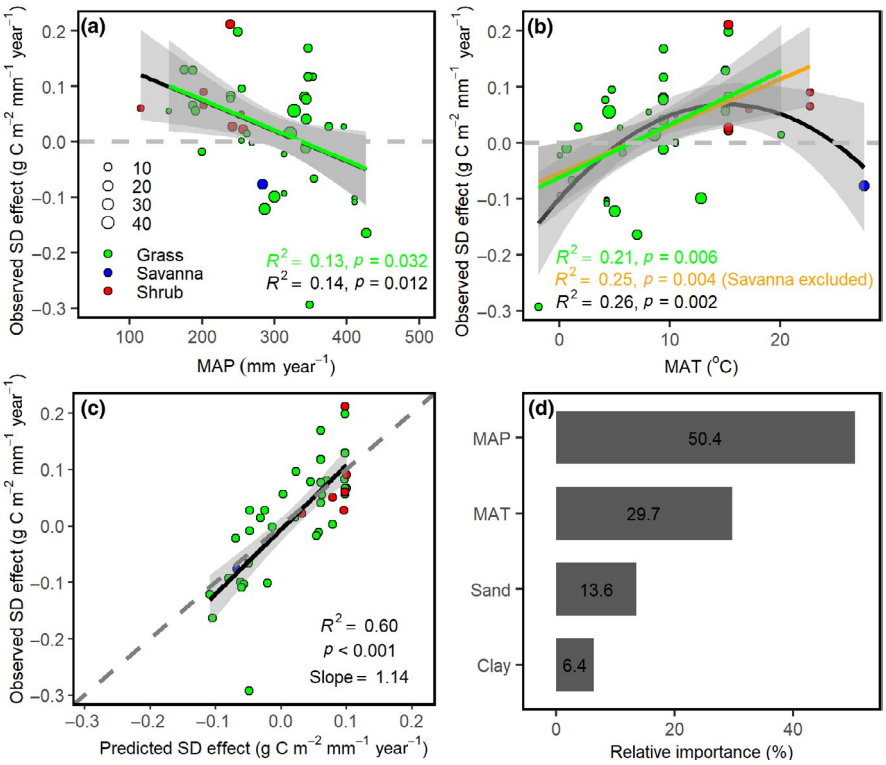

FIGURE 2 The effect of interannual precipitation variability on aboveground net primary production (ANPP) in relation to its predictors. The effect of interannual precipitation variability, indexed by the standard deviation (SD) of annual precipitation, on ANPP was a function of (a) mean annual precipitation (MAP) and (b) mean annual temperature (MAT). (c) The observed effect versus the effect predicted by a boosted regression tree model. (d) Relative importance of the predictors quantified using the boosted regression tree model. In (a,b), point size is proportional to sample size; the sample size-weighted regression line is given in grasslands (green) and across all sites (black, but orange when the only savanna site was excluded); the shaded band indicates the 95% confidence interval. In (c), the black line and the shaded band indicate the regression line and the 95% confidence interval, respectively. In (d), Sand and Clay indicate soil sand content and clay content, respectively [Colour figure can be viewed at wileyonlinelibrary.com]

MAP and the MAT gradients were probably related to the negative correlation between MAP and MAT ($r = -0.57$, $p < 0.001$; Figure 1b).

The effect of precipitation variability on ANPP did not differ significantly between grasslands and shrublands with similar MAP and MAT ($p > 0.05$; Figure 2a,b). Moreover, the effect was not significantly related to soil sand content ($r = 0.14$, $p = 0.40$) or clay content ($r = 0.15$, $p = 0.33$). BRT analysis, which explained 60% of the total variation in the effect (Figure 2c), confirmed that MAP and MAT were the most important predictors, while soil sand content and clay content were less important predictors (Figure 2d), and vegetation type was of minor importance and therefore excluded from the final BRT model. Relative importance of MAT and MAP in predicting effects of variability was indicated differently by the regression analysis and the BRT analysis, again, probably due to the collinearity between MAP and MAT (Figure 1b).

3.2 | Simulated effects of precipitation variability on ANPP and water fluxes

Our process-based model simulated comparable effects of precipitation variability on ANPP within the MAP range of the observational data (i.e., 116–427 mm year^{-1}), and showed that the simulated effect switched from positive to negative at about 300 mm year^{-1} MAP (Figure 3a). Moreover, modeling analysis identified a positive peak effect at about 140 mm year^{-1} MAP, which was not captured by the observational data (Figure 3a).

Importantly, our modeling analysis revealed the effects of precipitation variability on ecosystem water fluxes and water availability in the soil profile (Figure 3b,c). Increased precipitation variability altered the partitioning of precipitation into transpiration, evaporation, and water loss through runoff and drainage (Figure 3b). The effect of precipitation variability on transpiration mirrored that on ANPP (Figure 3a,b). The opposite pattern was generally true for the effect of precipitation variability on evaporation, which was consistently negative (Figure 3b). The effect of precipitation variability on water loss through runoff and drainage was consistently positive and increased gradually with increasing MAP (Figure 3b). Increased precipitation variability consistently decreased shallow soil (<5 cm depth) water availability and also decreased subsoil (>5 cm) water availability at MAP > 300 mm year^{-1}, but increased subsoil water availability at lower MAP (Figure 3c). The positive effect of precipitation variability on subsoil water availability peaked round 140 mm year^{-1}

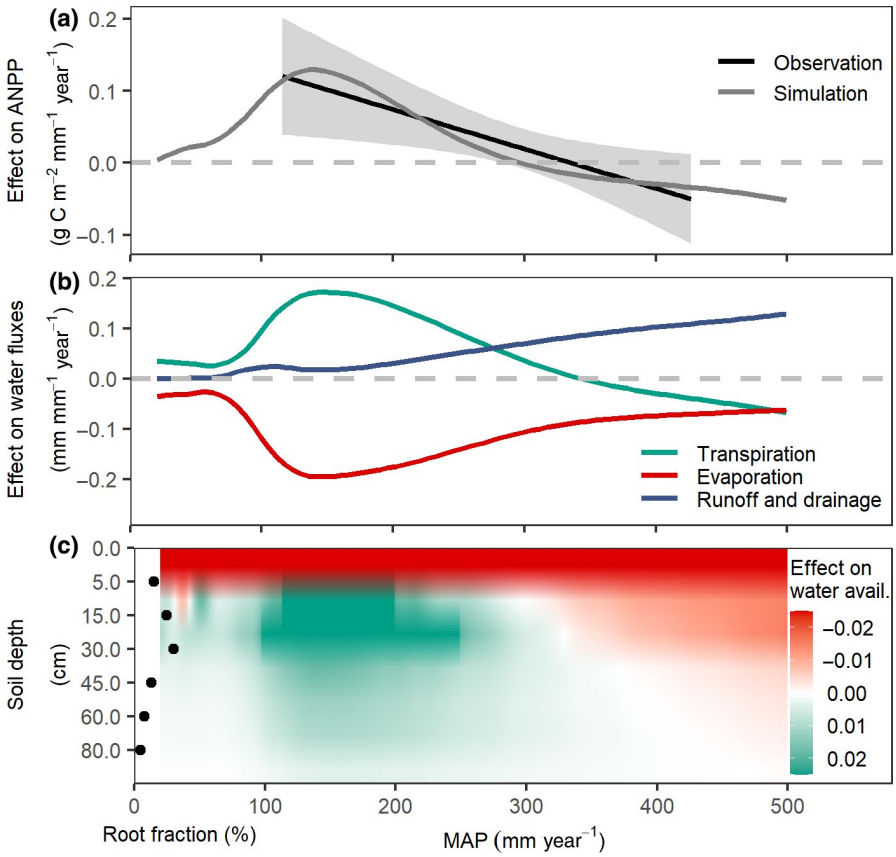

FIGURE 3 Hydraulic mechanism underlying the effect of interannual precipitation variability on aboveground net primary production (ANPP). (a) The effect of interannual precipitation variability on ANPP in model simulations (gray line) generally matched well with the effect calculated from long-term ANPP observations (black line and shaded band, as in Figure 2a) along the mean annual precipitation (MAP) gradient. In modeling analysis, (b) interannual precipitation variability affected ANPP mainly by altering the partitioning of precipitation into transpiration, evaporation, and loss from the ecosystem via runoff and drainage. (c) Interannual precipitation variability altered the partitioning of precipitation into transpiration and evaporation further by changing water availability in the soil profile (unit: mm mm^{-1} year^{-1}). In (c), the black point indicates the fraction of roots in each soil layer used in the model [Colour figure can be viewed at wileyonlinelibrary.com]

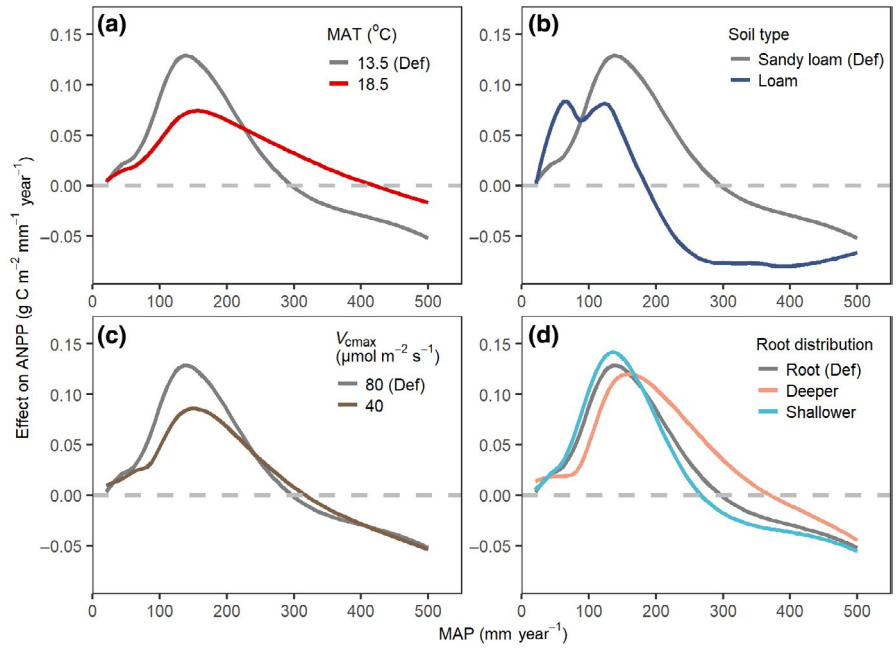

FIGURE 4 Simulated effect of interannual precipitation variability on aboveground net primary production (ANPP) is modulated by mean annual temperature (MAT), soil type, and plant physiological traits. (a) MAT; (b) soil type; (c) leaf maximum carboxylation rate (V_{cmax}); (d) root distribution in soil profile. In each subplot, the gray line indicates the effect simulated with the default parameter values, and the colored line(s) indicate the effect(s) simulated with the altered parameter value(s) [Colour figure can be viewed at wileyonlinelibrary.com]

MAP (Figure 3c), the same MAP value where the positive effects on transpiration and ANPP peaked.

When MAP was <230 mm year^{-1}, a higher MAT reduced ANPP (Figure S3a) and its sensitivity (i.e., less positive) to precipitation variability (Figure 4a). When MAP was higher than this threshold, higher MAT increased evaporation (Figure S3c) and decreased the effects of precipitation variability on evaporation and water loss through runoff and drainage (Figure S4a), resulting in more positive or less negative effects on transpiration (Figure S4a) and ANPP (Figure 4a). Sandy loam soil facilitates water infiltration and thus increased transpiration and ANPP over loam soil (Figure 4b; Figure S4b). In comparison to sandy loam soil, loam soil lost more water through surface

runoff (Figure S3d); meanwhile, loam soil had a larger water holding capacity (Table S3) and therefore should retain more water in the surface soil layer, which was depleted by evaporation (Figure S3c).

A decrease in V_{cmax} from 80 to 40 μmol m^{-2} s^{-1} reduced ANPP (Figure S3a) as well as its sensitivity to precipitation variability when MAP was <240 mm $year^{-1}$, but had little impact on sensitivity when MAP was higher than this threshold (Figure 4c). Shallow roots benefited more from increased precipitation variability at MAP < 170 mm $year^{-1}$, whereas deep roots benefited more or lost less at MAP > 170 mm $year^{-1}$ (Figure 4d).

3.3 | The effect of precipitation variability on ANPP in global drylands with MAP < 500 mm $year^{-1}$

The effect of precipitation variability on ANPP was positive in southwestern Australia, the Middle East, and northwestern China, and negative in central North America, southern Russia, and northeastern China (Figure 5a,b), in accordance with the MAP of these regions (Figure 1a). These projected spatial patterns were similar between extrapolation from the observations using the BRT method and predictions from the model simulations (Figure 5a,b; Figure S5a). An exception was in the hyper-arid Sahara region, where the effects predicted from the model simulations were generally minor, but the effects extrapolated from the observations were strong and positive (Figure 5a,b). This difference resulted from the linear change in the observed effect while a unimodal change in the simulated effect along the MAP gradient (Figure 3a).

Year-to-year variation in precipitation has increased over the past century and will further increase in the future in most global drylands, with large spatial variations (Figure 5c,d). There were also large variations in further changes in precipitation variability among models (Figure S6). Despite considerable uncertainties in our estimated ANPP responses to precipitation variability change (Figure S5b,c), there were some spatial patterns of the ANPP responses (Figure 5e,f). Given historical changes in precipitation variability (Figure 5c), ANPP increased in Mongolia, northwestern China, western Australia, and Arabia, and decreased in central North America, northeastern China, and central Australia (Figure 5e). These patterns will be enhanced by future changes in precipitation variability; that is, ANPP will generally increase in areas where ANPP has increased and decrease in areas where ANPP has decreased (Figure 5e,f). An exception was in inner Australia, where ANPP has increased (Figure 5e) but will decrease (Figure 5f) due to decrease in precipitation variability in the future (Figure 5d).

Overall, ANPP has increased by 16.1 ± 2.4 Tg C $year^{-1}$ and will increase by an additional 12.2 ± 5.8 Tg C $year^{-1}$ due to changes in precipitation variability in global drylands with MAP < 500 mm $year^{-1}$ (Figure 5g,h). ANPP has increased by 19.6 ± 4.4 Tg C $year^{-1}$ in arid lands and hyper-arid lands, changed little (−1.0 ± 1.0 Tg C $year^{-1}$) in semi-arid lands, and decreased by 2.5 ± 1.0 Tg C $year^{-1}$ in dry sub-humid lands due to historical changes in precipitation variability (Figure 5g). Given future changes in precipitation variability, we predict that ANPP will increase by an additional 15.2 ± 6.0 Tg C $year^{-1}$ in arid lands and hyper-arid lands, will change little in semi-arid lands (−0.9 ± 0.7 Tg C $year^{-1}$), and will decrease by an additional 2.1 ± 0.5 Tg C $year^{-1}$ in dry sub-humid lands (Figure 5h).

4 | DISCUSSION

4.1 | The effect of precipitation variability on ANPP and its predictors

The effect of precipitation variability on ANPP estimated based on our observations (between −0.29 and 0.21 g C m^{-2} mm^{-1} $year^{-1}$; Figure 2a) and modeling analyses (between −0.06 and 0.14 g C m^{-2} mm^{-1} $year^{-1}$; Figure 3a) were both comparable to the estimates by Gherardi and Sala (2019) (−0.18 to 0.16 g C m^{-2} mm^{-1} $year^{-1}$ at MAP < 500 mm $year^{-1}$, recalculated from ANPP change per unit of precipitation CV). While empirical estimates of the effect of precipitation SD or CV on ANPP may be influenced by possible covariates (e.g., MAP and MAT), our modeling analysis has produced comparable estimates with the covariates controlled and thus confirmed the empirical estimates. Our estimates were larger in magnitude than the estimates by Hsu et al. (2012) (−0.07 and 0 g C m^{-2} mm^{-1} $year^{-1}$ at MAP < 500 mm $year^{-1}$), in which a similar dataset but a different statistical method (partial derivative of a quadratic approximation) was used. Estimates in Hsu et al. (2012) may be less robust, because they were derived indirectly from the nonlinearity of the relationship between ANPP and precipitation at each site, which depends on the nonlinear function used, an approach that lacks statistical power due to small sample sizes. The effect of precipitation variability on ANPP estimated in our study and Gherardi and Sala (2019) was of the same magnitude as previously estimated effects of precipitation mean on ANPP in drylands (mostly between 0 and 0.60 (mean about 0.30) g C m^{-2} mm^{-1} $year^{-1}$) (Hu et al., 2018; Wilcox et al., 2017; Wu et al., 2011).

As predicted by our first hypothesis, the simulated effect of precipitation variability on ANPP showed a unimodal relationship, rather than a linear negative relationship, with MAP, with a positive peak at 140 mm $year^{-1}$ (Figure 3a). The peak was not revealed in prior analyses, which did not include the extremely dry conditions (MAP < 140 mm $year^{-1}$) (Gherardi & Sala, 2019; Heisler-White et al., 2008; Knapp et al., 2002; Thomey et al., 2011). This threshold was also not revealed in our observational data (Figure 2a), which included more sites with MAP < 230 mm $year^{-1}$ than Gherardi and Sala (2019) but with only one site at MAP < 140 mm $year^{-1}$. Nevertheless, observations in our study and Gherardi and Sala (2019) and our modeling analysis consistently showed that when MAP > 140 mm, the effect of precipitation variability on ANPP decreased gradually with increasing MAP. This result differs from Hsu et al. (2012), in which no significant change in the effect of precipitation variability along the MAP gradient was found.

As predicted by our second hypothesis, both our observations and modeling analysis showed that MAT modulated the effect of precipitation variability on ANPP. This result is in line with two

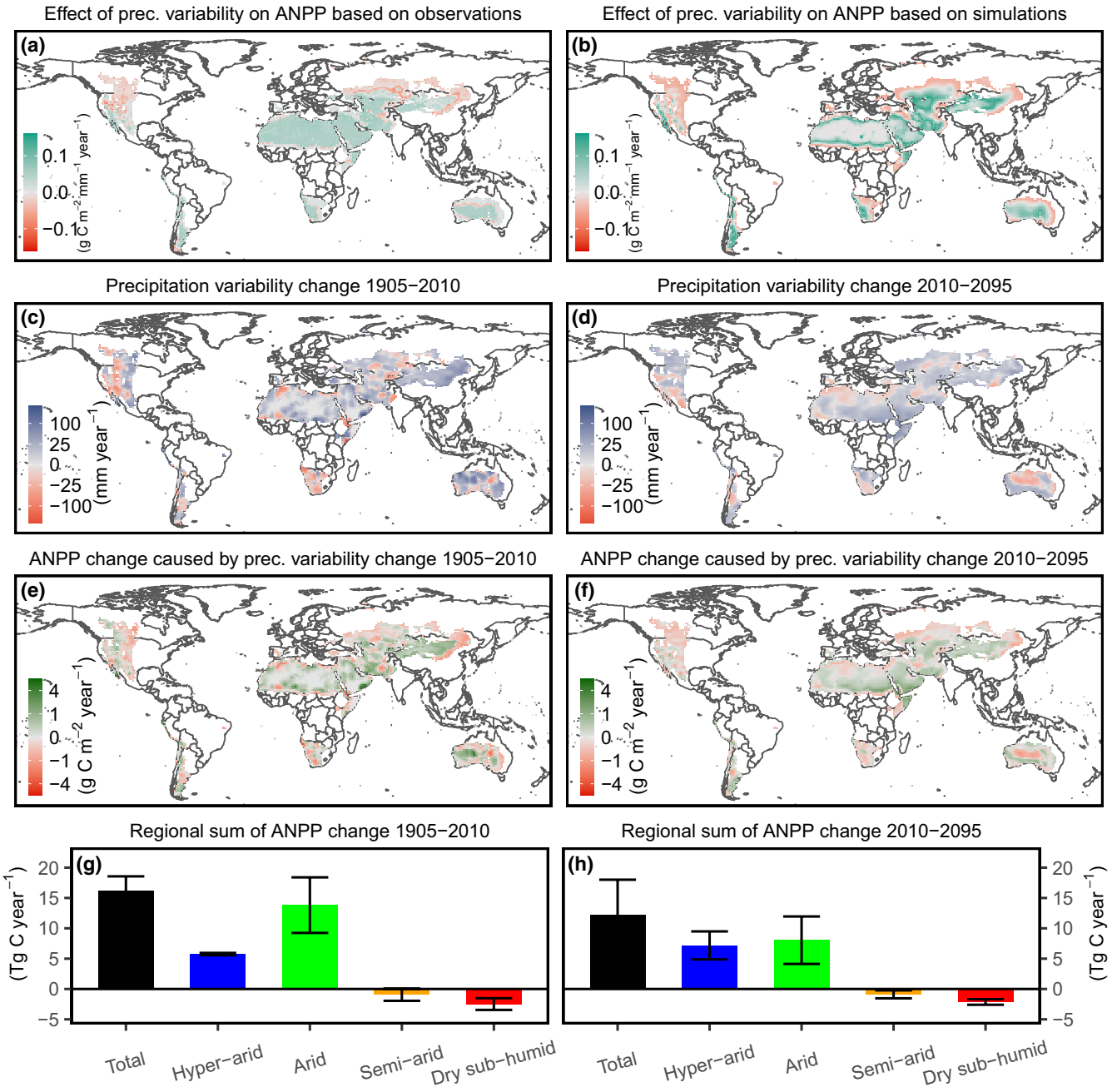

FIGURE 5 Global patterns of changes in interannual precipitation variability and their effects on aboveground net primary production (ANPP) in drylands with mean annual precipitation <500 mm year^{-1}. The effect of interannual precipitation variability on ANPP estimated based on (a) observations and (b) model simulations, respectively. Changes in interannual precipitation variability during (c) 1905–2010 and (d) 2010–2095, respectively. Ensemble mean ANPP changes caused by changes in interannual precipitation variability during (e) 1905–2010 and (f) 2010–2095, respectively. ANPP changes caused by changes in interannual precipitation variability in different types of drylands during (g) 1905–2010 and (h) 2010–2095, respectively. In (g,h), error bar indicates standard error [Colour figure can be viewed at wileyonlinelibrary.com]

recent studies (Liu et al., 2020; Rudgers et al., 2018). Rudgers et al. (2018) suggested that rising temperature in drylands can modulate the effect of interannual precipitation variability on ANPP, based on an analysis of 12–15 years of ANPP and climate measurements at three Sevilleta sites. Liu et al. (2020) found that more extreme precipitation regimes positively affected ANPP in a warm grassland (MAT 13.2°C) at Sevilleta but negatively affected ANPP in a cold grassland (MAT −0.5°C) in Inner Mongolia, China, where MAP (250 vs. 358 mm year^{-1}) and soil texture (68% vs. 60% sand, 10% vs. 21% clay) are similar.

Soil type and plant physiological traits also modulated the effect of precipitation variability on ANPP. Theory predicts that soil type or soil particle size can mediate the effect of precipitation variability on primary production, because it can affect infiltration and soil water

holding capacity (Sala et al., 2015). This hypothesis is confirmed by our modeling analysis but not by our observations, probably because gap-filled data of soil particle size were inaccurate. Similarly, whether vegetation type can influence the effect of precipitation variability on ANPP cannot be rigorously tested by our observations due to limited sample sizes in shrubland and savanna, but it was suggested to be significant by our modeling analyses with alternative leaf V_{cmax} and soil-profile root distribution. Our modeling results (Figure 4c,d) support the hypothesis that vegetation type can modulate the effect of precipitation variability on ANPP through plant physiological traits (Griffin-Nolan et al., 2019; Rudgers et al., 2018).

4.2 | Mechanisms underlying the effect of precipitation variability on ANPP

Consistent with our third hypothesis, our modeling analysis revealed that the primary mechanism underlying the effect of precipitation variability on ANPP lies in how precipitation is partitioned into transpiration for plant growth versus water loss through evaporation, runoff, and drainage. The positive peak of the effect at 140 mm year^{-1} MAP was because that sites with ~140 mm year^{-1} MAP supported the optimum percolation depth (5–30 cm) for maximal plant growth (Figure 3c). The small response of ANPP to increased precipitation variability at extremely dry sites (MAP < 140 mm year^{-1}) is in line with the meristem constraints hypothesis (Dalgleish & Hartnett, 2006; Reichmann et al., 2013), which states that in extremely dry year or site meristem density constrains ANPP and its sensitivity to precipitation by limiting recruitment of new meristems. At sites with MAP <300 mm year^{-1}, ecosystem water loss through runoff and drainage was minimal (Figure S3d). Increased precipitation variability increased water availability of the subsoil where it was depleted mainly by plants via transpiration, and correspondingly decreased water availability of the shallow soil where it was lost primarily by evaporation (Figure 3b,c). At wetter sites (MAP ≥ 300 mm year^{-1}), a significant proportion of precipitation was lost through runoff and drainage (Figure S3d). Increased precipitation variability resulted in disproportionately greater water loss through runoff and drainage in wet years or sites than in dry years or sites (Figure S3d). Consequently, at these sites, the partitioning of precipitation into transpiration for plant growth was reduced as precipitation variability increased (Figure 3b).

MAT, soil type, and plant physiological traits all altered the magnitude but not the pattern of the simulated effect of precipitation variability on ANPP along the MAP gradient. A positive impact of MAT on the effect of precipitation variability on ANPP has been suggested by our observations, and also by our modeling analysis at MAP > 230 mm year^{-1}. The positive MAT impact could occur because hot climates drive more water loss through evaporation, making plants benefit more or lose less from variable precipitation patterns that recharge subsoil water (Liu et al., 2020; Rudgers et al., 2018). This mechanism is important when the partitioning of precipitation into evaporation is low, but not when the partition is already very high (i.e., close to 100%), as observed at very dry and hot sites (Figure S3b,c; Sala et al., 2015). At very dry and hot sites, high temperature can reduce leaf photosynthetic rate directly due to the temperature effect on photosynthesis and indirectly by further reducing soil water availability (Duffy et al., 2021; Quan et al., 2019), which probably explains why high MAT reduced the simulated effect of precipitation variability on ANPP at MAP < 230 mm year^{-1} (Figure 4a). Such a negative MAT impact was not revealed by our observational data ($p = 0.16$, $n = 9$, at MAP < 230 mm year^{-1}), probably because of lack of statistical power. As expected, our modeling analysis showed that the sandy loam soil facilitated water infiltration and plant growth over the loam soil under increased precipitation variability in the dry conditions we explored (Figure 4b). The inverse texture hypothesis predicts that in wetter conditions ANPP on sandy loam soil may be reduced more by increased precipitation variability than that on loam soil, due to more water lose from sandy loam soil through drainage (Sala et al., 1988, 2015).

The interaction between plant physiological traits and MAP modulated the effect of precipitation variability on ANPP. When MAP was <240 mm year^{-1}, decreased leaf V_{cmax} reduced ANPP (Figure S3a) and its sensitivity to precipitation variability (Figure 4c), which is consistent with previous studies at dry sites that showed more benefits of plants with a fast growth rate from variable precipitation than plants with a slower growth rate (Rudgers et al., 2018; Xu et al., 2015). At wetter sites (MAP > 240 mm year^{-1}), decreased V_{cmax}, however, did not lead to a smaller negative effect on ANPP (Figure 4c), probably because of more water loss through drainage at increased precipitation variability (Figure S3d). As precipitation variability increased, shallow roots promoted plant growth more than deep roots at low MAP < 170 mm year^{-1}, whereas deep roots benefited more or lost less than shallow roots at higher MAP (Figure 4d), probably because water infiltrates to deeper soil layers with increasing MAP and precipitation variability. Similarly, previous studies on drylands with MAP > 170 mm year^{-1} have shown that increased interannual precipitation variability promoted the production of deep-rooted shrub or tree species but decreased that of shallow-rooted grass species (Gherardi & Sala, 2015; Rudgers et al., 2018; Xu et al., 2015).

4.3 | Global patterns of precipitation variability effect on ANPP

Our results showed widespread but heterogeneous responses of ANPP to changes in precipitation variability both historically and in the future (Figure 5e,f). The heterogeneous responses were attributed to both spatial heterogeneity in the effect of precipitation variability on ANPP (Figure 5a,b) and spatial heterogeneity in precipitation variability change (Figure 5c,d). Spatial heterogeneity in the effect size was further ascribed to spatial heterogeneities in MAP, MAT, and soil particle size (Figure 2d). Our prediction models did not include potential predictors such as community structure, plant diversity, nutrients, disturbances (e.g., fire), and intra-annual variability in precipitation (Fay et al., 2015; Knapp, Carroll, et al., 2015; Liu

et al., 2020; Rudgers et al., 2018; Sala et al., 2015; Yu et al., 2017), and therefore could underestimate spatial heterogeneity in the effect size. Spatial heterogeneity in precipitation variability change could also be underestimated due to the "coarse-graining problem," where heterogeneities with spatial grids are lost through spatial averaging (Newman et al., 2019). Therefore, spatial heterogeneities in ANPP response to precipitation variability change revealed in our study are conservative.

Uncertainties in our estimates of ANPP response to precipitation variability change could be large, due to several reasons. First, as stated above, we did not include some potential predictors in our models. Second, we assumed that only precipitation variability has changed in the past or will change in the future, while other environmental factors (e.g., MAP, MAT, and atmospheric CO_2 concentration) and ecosystem properties (e.g., community structure and nutrients) are constant during the studied periods. Finally, when predicted to the future, additional uncertainties were introduced by uncertainties in future changes in precipitation variability (Figure S6). Therefore, our global patterns of ANPP response to precipitation variability change may be considered as working hypotheses to be tested by future long-term precipitation manipulation experiments and long-term ANPP observations. Despite these uncertainties, our global estimate of ANPP response to future precipitation variability (12.2 ± 5.8 Tg C year^{-1}) is improved compared with the estimate by Gherardi and Sala (2019) (−100 to −300 Tg C year^{-1}), in which neither spatial heterogeneity in precipitation variability effect on ANPP nor spatial heterogeneity in precipitation variability change was considered (i.e., averages were used). The large difference in the two global estimates could be also because of the different MAP ranges used between our study (<500 mm year^{-1}) and their study (up to >1,000 mm year^{-1}).

5 | CONCLUSION

Our results suggest that changes in precipitation variability have a net positive impact on primary production when integrated across global drylands with MAP < 500 mm year^{-1}. Future increases in precipitation variability will likely increase primary production in arid and hyper-arid ecosystems but will decrease primary production in dry sub-humid lands. The primary mechanism underlying ANPP responses to changes in precipitation variability is how precipitation is partitioned into runoff, drainage, and percolation into shallow soil versus subsoil layers, which also varies with ecosystem properties and climate conditions. These results suggest that primary production will respond differently to future precipitation variability in global drylands as a function of both environmental factors and ecosystem properties.

ACKNOWLEDGMENTS

We thank Xingjie Lu for his help with programming and the three anonymous reviewers for their suggestions and comments. This work was supported by grants from the National Science Foundation for Long-term Ecological Research including DEB 1748133 and 1655499 as well as DOE Ameriflux (to Litvak).

CONFLICT OF INTEREST

The authors declare no competing interests.

AUTHOR CONTRIBUTIONS

Y.L., J.R., and E.H. designed the study. M.L. provided eddy flux measurements and ANPP data at Sevilleta. E.H. compiled the literature data, ran model simulations, and performed the statistical analyses, with contributions from Y.L. and J.R. E.H. wrote the initial manuscript, with substantial input from Y.L., J.R., S.C., M.L., J.L., W.P., D.H. and S.N. All authors edited and approved the manuscript.

DATA AVAILABILITY STATEMENT

The data and code supporting the findings of this study are available at Figshare (https://doi.org/10.6084/m9.figshare.13020695.v1).

ORCID

Enqing Hou https://orcid.org/0000-0003-4864-2347
Marcy E. Litvak https://orcid.org/0000-0002-4255-2263
Jennifer A. Rudgers https://orcid.org/0000-0001-7094-4857
Scott L. Collins https://orcid.org/0000-0002-0193-2892
William T. Pockman https://orcid.org/0000-0002-3286-0457
Dafeng Hui https://orcid.org/0000-0002-5284-2897
Shuli Niu https://orcid.org/0000-0002-2394-2864

REFERENCES

Ahlström, A., Raupach, M. R., Schurgers, G., Smith, B., Arneth, A., Jung, M., Reichstein, M., Canadell, J. G., Friedlingstein, P. & Jain, A. K. (2015). The dominant role of semi-arid ecosystems in the trend and variability of the land CO_2 sink. *Science*, *348*(6237), 895–899.

Bivand, R., & Piras, G. (2015). Comparing implementations of estimation methods for spatial econometrics. *Journal of Statistical Software*, *63*(18), 1–36.

Borgogno, F., D'Odorico, P., Laio, F., & Ridolfi, L. (2007). Effect of rainfall interannual variability on the stability and resilience of dryland plant ecosystems. *Water Resources Research*, *43*(6), W06411.

Chen, N., Jayaprakash, C., Yu, K., & Guttal, V. (2018). Rising variability, not slowing down, as a leading indicator of a stochastically driven abrupt transition in a dryland ecosystem. *The American Naturalist*, *191*(1), E1–E14.

Dalgleish, H. J., & Hartnett, D. C. (2006). Below-ground bud banks increase along a precipitation gradient of the North American Great Plains: A test of the meristem limitation hypothesis. *New Phytologist*, *171*(1), 81–89.

Duffy, K. A., Schwalm, C. R., Arcus, V. L., Koch, G. W., Liang, L. L., & Schipper, L. A. (2021). How close are we to the temperature tipping point of the terrestrial biosphere? *Science Advances*, *7*(3), eaay1052. https://doi.org/10.1126/sciadv.aay1052

EcoTrends database. (2004). Retrieved June 30, 2019 from https://ecotrends.info/

Elith, J., Leathwick, J. R., & Hastie, T. (2008). A working guide to boosted regression trees. *The Journal of Animal Ecology*, *77*(4), 802–813. https://doi.org/10.1111/j.1365-2656.2008.01390.x

Fay, P. A., Prober, S. M., Harpole, W. S., Knops, J. M. H., Bakker, J. D., Borer, E. T., Lind, E. M., MacDougall, A. S., Seabloom, E. W., Wragg, P. D., Adler, P. B., Blumenthal, D. M., Buckley, Y. M., Chu, C., Cleland,

E. E., Collins, S. L., Davies, K. F., Du, G., Feng, X., … Yang, L. H. (2015). Grassland productivity limited by multiple nutrients. *Nature Plants*, *1*(7), 15080. https://doi.org/10.1038/nplants.2015.80

Felton, A. J., Knapp, A. K., & Smith, M. D. (2021). Precipitation–productivity relationships and the duration of precipitation anomalies: An underappreciated dimension of climate change. *Global Change Biology*, *27*(6), 1127–1140. https://doi.org/10.1111/gcb.15480

Fick, S. E., & Hijmans, R. J. (2017). WorldClim 2: new 1-km spatial resolution climate surfaces for global land areas. *International Journal of Climatology*, *37*(12), 4302–4315. https://doi.org/10.1002/joc.5086

Gherardi, L. A., & Sala, O. E. (2015). Enhanced precipitation variability decreases grass- and increases shrub-productivity. *Proceedings of the National Academy of Sciences of the United States of America*, *112*(41), 12735–12740. https://doi.org/10.1073/pnas.1506433112

Gherardi, L. A., & Sala, O. E. (2019). Effect of inter-annual precipitation variability on dryland productivity: A global synthesis. *Global Change Biology*, *25*, 269–276. https://doi.org/10.1111/gcb.14480

Griffin-Nolan, R. J., Blumenthal, D. M., Collins, S. L., Farkas, T. E., Hoffman, A. M., Mueller, K. E., Ocheltree, T. W., Smith, M. D., Whitney, K. D., & Knapp, A. K. (2019). Shifts in plant functional composition following long-term drought in grasslands. *Journal of Ecology*, *107*(5), 2133–2148. https://doi.org/10.1111/1365-2745.13252

Harris, I., Jones, P. D., Osborn, T. J., & Lister, D. H. (2014). Updated high-resolution grids of monthly climatic observations–the CRU TS3.10 Dataset. *International Journal of Climatology*, *34*(3), 623–642. https://doi.org/10.1002/joc.3711

Haverd, V., Ahlström, A., Smith, B., & Canadell, J. G. (2017). Carbon cycle responses of semi-arid ecosystems to positive asymmetry in rainfall. *Global Change Biology*, *23*(2), 793–800.

Heisler-White, J. L., Blair, J. M., Kelly, E. F., Harmoney, K., & Knapp, A. K. (2009). Contingent productivity responses to more extreme rainfall regimes across a grassland biome. *Global Change Biology*, *15*(12), 2894–2904.

Heisler-White, J. L., Knapp, A. K., & Kelly, E. F. (2008). Increasing precipitation event size increases aboveground net primary productivity in a semi-arid grassland. *Oecologia*, *158*(1), 129–140.

Hsu, J. S., Powell, J., & Adler, P. B. (2012). Sensitivity of mean annual primary production to precipitation. *Global Change Biology*, *18*(7), 2246–2255.

Hu, Z., Guo, Q., Li, S., Piao, S., Knapp, A. K., Ciais, P., & Yu, G. (2018). Shifts in the dynamics of productivity signal ecosystem state transitions at the biome-scale. *Ecology Letters*, *21*(10), 1457–1466.

Huxman, T. E., Smith, M. D., Fay, P. A., Knapp, A. K., Shaw, M. R., Loik, M. E., Smith, S. D., Tissue, D. T., Zak, J. C., Weltzin, J. F., Pockman, W. T., Sala, O. E., Haddad, B. M., Harte, J., Koch, G. W., Schwinning, S., Small, E. E., & Williams, D. G. (2004). Convergence across biomes to a common rain-use efficiency. *Nature*, *429*, 651–654. https://doi.org/10.1038/nature02561

Jiang, J., Huang, Y., Ma, S., Stacy, M., Shi, Z., Ricciuto, D. M., & Luo, Y. (2018). Forecasting responses of a northern peatland carbon cycle to elevated CO_2 and a gradient of experimental warming. *Journal of Geophysical Research: Biogeosciences*, *123*(3), 1057–1071.

Knapp, A. K., Beier, C., Briske, D. D., Classen, A. T., Luo, Y., Reichstein, M., Smith, M. D., Smith, S. D., Bell, J. E., Fay, P. A., Heisler, J. L., Leavitt, S. W., Sherry, R., Smith, B., & Weng, E. (2008). Consequences of more extreme precipitation regimes for terrestrial ecosystems. *BioScience*, *58*(9), 811–821. https://doi.org/10.1641/B580908

Knapp, A. K., Carroll, C. J. W., Denton, E. M., La Pierre, K. J., Collins, S. L., & Smith, M. D. (2015). Differential sensitivity to regional-scale drought in six central US grasslands. *Oecologia*, *177*(4), 949–957. https://doi.org/10.1007/s00442-015-3233-6

Knapp, A. K., Ciais, P., & Smith, M. D. (2017). Reconciling inconsistencies in precipitation-productivity relationships: implications for climate change. *New Phytologist*, *214*(1), 41–47. https://doi.org/10.1111/nph.14381

Knapp, A. K., Fay, P. A., Blair, J. M., Collins, S. L., Smith, M. D., Carlisle, J. D., & McCarron, J. K. (2002). Rainfall variability, carbon cycling, and plant species diversity in a mesic grassland. *Science*, *298*(5601), 2202–2205.

Knapp, A. K., Hoover, D. L., Wilcox, K. R., Avolio, M. L., Koerner, S. E., La Pierre, K. J., Loik, M. E., Luo, Y., Sala, O. E., & Smith, M. D. (2015). Characterizing differences in precipitation regimes of extreme wet and dry years: implications for climate change experiments. *Global Change Biology*, *21*(7), 2624–2633. https://doi.org/10.1111/gcb.12888

Liu, J., Ma, X., Duan, Z., Jiang, J., Reichstein, M., & Jung, M. (2020). Impact of temporal precipitation variability on ecosystem productivity. *WIREs Water*, *7*(6), e1481. https://doi.org/10.1002/wat2.1481

Long Term Ecological Research Network. (2016). Retrieved June 30, 2019 from https://environmentaldatainitiative.org/

Luo, Y., Jiang, L., Niu, S., & Zhou, X. (2017). Nonlinear responses of land ecosystems to variation in precipitation. *New Phytologist*, *214*(1), 5–7. https://doi.org/10.1111/nph.14476

Maurer, G. E., Hallmark, A. J., Brown, R. F., Sala, O. E., & Collins, S. L. (2020). Sensitivity of primary production to precipitation across the United States. *Ecology Letters*, *23*, 527–536. https://doi.org/10.1111/ele.13455

Meng, B., Li, J., Zhong, S., Maurer, G., Yao, Y., Yang, X., Collins, S., & Sun, W. (2021). Nitrogen addition amplifies the nonlinear drought response of grassland productivity to extended growing-season droughts. *Ecology*, in press.

Newman, E. A., Kennedy, M. C., Falk, D. A., & McKenzie, D. (2019). Scaling and complexity in landscape ecology. *Frontiers in Ecology and Evolution*, *7*, 293. https://doi.org/10.3389/fevo.2019.00293

Oak Ridge National Laboratory Distributed Active Archive Center. (2009). Retrieved June 30, 2019 from https://daac.ornl.gov/get_data/

Paschalis, A., Fatichi, S., Zscheischler, J., Ciais, P., Bahn, M., Boysen, L., & Zhu, Q. (2020). Rainfall manipulation experiments as simulated by terrestrial biosphere models: Where do we stand? *Global Change Biology*, *26*, 3190–3192.

Poulter, B., Frank, D., Ciais, P., Myneni, R. B., Andela, N., Bi, J., Broquet, G., Canadell, J. G., Chevallier, F., Liu, Y. Y., Running, S. W., Sitch, S., & van der Werf, G. R. (2014). Contribution of semi-arid ecosystems to interannual variability of the global carbon cycle. *Nature*, *509*, 600–603. https://doi.org/10.1038/nature13376

Prăvălie, R. (2016). Drylands extent and environmental issues. A global approach. *Earth-Science Reviews*, *161*, 259–278. https://doi.org/10.1016/j.earscirev.2016.08.003

Quan, Q., Tian, D., Luo, Y., Zhang, F., Crowther, T. W., Zhu, K., Chen, H. Y. H., Zhou, Q., & Niu, S. (2019). Water scaling of ecosystem carbon cycle feedback to climate warming. *Science Advances*, *5*(8), eaav1131. https://doi.org/10.1126/sciadv.aav1131

R Core Team (2020). *R: A language and environment for statistical computing*. R Foundation for Statistical Computing. http://www.R-project.org/

Reichmann, L. G., Sala, O. E., & Peters, D. P. (2013). Precipitation legacies in desert grassland primary production occur through previous-year tiller density. *Ecology*, *94*(2), 435–443. https://doi.org/10.1890/12-1237.1

Rudgers, J. A., Chung, Y. A., Maurer, G. E., Moore, D. I., Muldavin, E. H., Litvak, M. E., & Collins, S. L. (2018). Climate sensitivity functions and net primary production: A framework for incorporating climate mean and variability. *Ecology*, *99*(3), 576–582.

Ryel, R., Caldwell, M., Yoder, C., Or, D., & Leffler, A. (2002). Hydraulic redistribution in a stand of Artemisia tridentata: Evaluation of benefits to transpiration assessed with a simulation model. *Oecologia*, *130*(2), 173–184.

Sala, O. E., Gherardi, L. A., & Peters, D. P. C. (2015). Enhanced precipitation variability effects on water losses and ecosystem functioning:

Differential response of arid and mesic regions. *Climatic Change*, *131*(2), 213–227.

Sala, O. E., Gherardi, L. A., Reichmann, L., Jobbagy, E., & Peters, D. (2012). Legacies of precipitation fluctuations on primary production: Theory and data synthesis. *Philosophical Transactions of the Royal Society of London B: Biological Sciences*, *367*(1606), 3135–3144.

Sala, O. E., Parton, W. J., Joyce, L., & Lauenroth, W. (1988). Primary production of the central grassland region of the United States. *Ecology*, *69*(1), 40–45.

Seneviratne, S. I., Nicholls, N., Easterling, D., Goodess, C. M., Kanae, S., Kossin, J., Luo, Y., Marengo, J., McInnes, K., Rahimi, M., Reichstein, M., Sorteberg, A., Vera, C., & Zhang, X. (2012). Changes in climate extremes and their impacts on the natural physical environment. In C. B. Field, V. Barros, T. F. Stocker, D. Qin, D. J. Dokken, K. L. Ebi, M. D. Mastrandrea, K. J. Mach, G.-K. Plattner, S. K. Allen, M. Tignor, & P. M. Midgley (Eds.), *Managing the risks of extreme events and disasters to advance climate change adaptation* (pp. 109–230). Cambridge University Press.

Stocker, T. F. (2013). *Climate change 2013: The physical science basis: Working Group I Contribution to the Fifth Assessment Report of the Intergovernmental Panel on Climate Change*. Cambridge University Press.

Taylor, K. E., Stouffer, R. J., & Meehl, G. A. (2012). An overview of CMIP5 and the experiment design. *Bulletin of the American Meteorological Society*, *93*(4), 485–498. https://doi.org/10.1175/BAMS-D-11-00094.1

Thomey, M. L., Collins, S. L., Vargas, R., Johnson, J. E., Brown, R. F., Natvig, D. O., & Friggens, M. T. (2011). Effect of precipitation variability on net primary production and soil respiration in a Chihuahuan Desert grassland. *Global Change Biology*, *17*(4), 1505–1515. https://doi.org/10.1111/j.1365-2486.2010.02363.x

UNEP-WCMC (2007). *A spatial analysis approach to the global delineation of dryland areas of relevance to the CBD Programme of Work on Dry and Subhumid Lands*. UNEP World Conservation Monitoring Centre.

Weng, E. S., & Luo, Y. Q. (2008). Soil hydrological properties regulate grassland ecosystem responses to multifactor global change: A modeling analysis. *Journal of Geophysical Research-Biogeosciences*, *113*, G03003. https://doi.org/10.1029/2007JG000539

Wieder, W. R., Boehnert, J., Bonan, G. B., & Langseth, M. (2014). *Regridded harmonized world soil database v1.2*. http://daac.ornl.gov/cgi-bin/dsviewer.pl?ds_id=1247

Wilcox, K. R., Shi, Z., Gherardi, L. A., Lemoine, N. P., Koerner, S. E., Hoover, D. L., Bork, E., Byrne, K. M., Cahill, J., Collins, S. L., Evans, S., Gilgen, A. K., Holub, P., Jiang, L., Knapp, A. K., LeCain, D., Liang, J., Garcia-Palacios, P., Peñuelas, J., … Luo, Y. (2017). Asymmetric responses of primary productivity to precipitation extremes: A synthesis of grassland precipitation manipulation experiments. *Global Change Biology*, *23*(10), 4376–4385. https://doi.org/10.1111/gcb.13706

Wu, Z., Dijkstra, P., Koch, G. W., Peñuelas, J., & Hungate, B. A. (2011). Responses of terrestrial ecosystems to temperature and precipitation change: A meta-analysis of experimental manipulation. *Global Change Biology*, *17*(2), 927–942. https://doi.org/10.1111/j.1365-2486.2010.02302.x

Xu, X. T., Medvigy, D., & Rodriguez-Iturbe, I. (2015). Relation between rainfall intensity and savanna tree abundance explained by water use strategies. *Proceedings of the National Academy of Sciences of the United States of America*, *112*(42), 12992–12996. https://doi.org/10.1073/pnas.1517382112

Yu, K. L., Saha, M. V., & D'Odorico, P. (2017). The effects of interannual rainfall variability on tree-grass composition along Kalahari rainfall gradient. *Ecosystems*, *20*(5), 975–988. https://doi.org/10.1007/s10021-016-0086-8

SUPPORTING INFORMATION

Additional supporting information may be found online in the Supporting Information section.

How to cite this article: Hou, E., Litvak, M. E., Rudgers, J. A., Jiang, L., Collins, S. L., Pockman, W. T., Hui, D., Niu, S., & Luo, Y. (2021). Divergent responses of primary production to increasing precipitation variability in global drylands. *Global Change Biology*, 27, 5225–5237. https://doi.org/10.1111/gcb.15801